Animation of Drift Ballooning Modes and Zonal Flow Turbulence

J. Candy, R.E. Waltz and M.N. Rosenbluth
General Atomics
San Diego, California 92186
USA

42nd APS (DPP) Meeting
Québec, Québec, CANADA
23-27 October 2000

Introduction

GENERAL ATOMICS

The Gyrokinetic-Maxwell (GKM) equations lay a firm but computationally challenging foundation for the investigation of microinstabilities and anomalous transport in fusion plasmas.

This poster describes *GYRO* – a nonlinear, electromagnetic, finite-β gyrokinetic code that incorporates a grid representative of real tokamak geometry.

Eventually, *GYRO* will contain all physics of low-frequency ($\omega < \omega_{ci}$) plasma turbulence, assuming only that the ion gyroradius is less than the magnetic field gradient length.

Introduction

GENERAL ATOMICS

The decision to pursue a full-radius code was made in order to

- ▷ quantify avalanches and action-at-a-distance effects;
- ▷ describe finite-ρ_* diamagnetic velocity shear stabilization of turbulence, where $\rho_* \equiv \rho/a$; and
- ▷ capture enough physics so that comparison of thermal diffusivities obtained from simulation can be directly compared with experiment.

Introduction

GENERAL ATOMICS

GYRO is distinguished from existing full-radius microinstability codes by its continuum approach, which solves the GKM equations on a fixed 5-dimensional grid rather than along characteristics (particle approach).

The perceived advantages of the continuum method are:

- ▷ implicit treatment of electron parallel motion, and
- ▷ absence of statistical noise in long-time solutions.

The perceived disadvantage is the substantially increased algorithmic and coding complexity.

Introduction

GENERAL ATOMICS

GYRO is also radially non-spectral, unlike existing continuum microinstability codes. A radial grid is used in place of $k_r = -i\partial/\partial r$, so that eventually a finite Δr-annulus with nonperiodic radial boundary conditions and finite-ρ_* may be simulated. This is much more difficult than the usual spectral approach using flux tubes, since the spectrum of 1D linear modes become a 2D mode for a given n.

In the first stage of code operation and validation reported here, profile variation is turned off and periodic radial boundary conditions are used to benchmark with the spectral, vanishing-ρ_* flux-tube codes *GKS* and *GS2*. This paper is a report on the first stage. The second stage will operate with realistic nonperiodic radial boundary conditions, general profile variation, and internal $n = 0$ sources (to prevent profile relaxation).

Model Equations

GENERAL ATOMICS

Using action-variational methods [Littlejohn], one can derive the guiding-center equations of motion including lowest-order drift effects

$$\dot{\mathbf{R}} = \frac{1}{B_{\|}^*}\left(v_{\|}\mathbf{B}^* - c\,\hat{\mathbf{b}}\times\mathbf{E}^*\right), \tag{1}$$

$$\dot{W} = \frac{e}{m}\frac{v_{\|}}{B_{\|}^*}\mathbf{B}^*\cdot\mathbf{E}^*, \tag{2}$$

where $v_{\|} \equiv \hat{\mathbf{b}}\cdot\dot{\mathbf{R}} = v_{\|}(\mathbf{R}, W, \mu)$ and $B_{\|}^* \equiv \hat{\mathbf{b}}\cdot\mathbf{B}^*$. The starred fields, with $\mathbf{A}^* \equiv \mathbf{A} + mcv_{\|}\hat{\mathbf{b}}/e$, are

$$\mathbf{B}^* \equiv \nabla\times\langle\mathbf{A}^*\rangle \qquad \text{and} \qquad \mathbf{E}^* \equiv -\nabla\langle\phi\rangle - \frac{1}{c}\frac{\partial\langle\mathbf{A}^*\rangle}{\partial t}. \tag{3}$$

Model Equations

GENERAL ATOMICS

$\mathbf{R} = \mathbf{x} - \boldsymbol{\rho}$ is the guiding center position, W is the unperturbed energy, and μ is the (conserved) magnetic moment. Angle brackets indicate gyroaverages. The conservative form of the gyrokinetic equation (with F the total guiding center distribution) follows automatically

$$\frac{\partial}{\partial t}\left(\mathcal{J}F\right) + \frac{\partial}{\partial \mathbf{R}}\left(\dot{\mathbf{R}}\mathcal{J}F\right) + \frac{\partial}{\partial W}\left(\dot{W}\mathcal{J}F\right) = 0\,. \tag{4}$$

$\mathcal{J} \equiv (v/v_{\parallel})B^{*}_{\parallel}$ is the velocity-space Jacobian. The perturbed B-field is

$$\delta\mathbf{B} = \nabla A_{\parallel} \times \hat{\mathbf{b}} + A_{\parallel}\nabla \times \hat{\mathbf{b}} \simeq \nabla A_{\parallel} \times \hat{\mathbf{b}} + \frac{A_{\parallel}}{B}\hat{\mathbf{b}} \times \nabla B \tag{5}$$

where $\mathbf{A} = \mathbf{A}_0 + A_{\parallel}\hat{\mathbf{b}}$. The approximate equality is valid in the limit of low-β. According to the gyrokinetic ordering, the second term in Eq. (5) is smaller than the first. It is therefore ignored in the kinetic equation, as are terms containing $\partial\hat{\mathbf{b}}/\partial t$.

Model Equations

GENERAL ATOMICS

Now, take $\hat{\mathbf{b}}$ along the equilibrium field. Then,

$$\frac{\partial F}{\partial t} + \mathbf{v}_\mathrm{g} \cdot \frac{\partial F}{\partial \mathbf{R}} - \frac{e}{m}\left(\mathbf{v}_\mathrm{g} \cdot \nabla \langle \phi \rangle + \frac{v_\parallel}{c}\frac{\partial \langle A_\parallel \rangle}{\partial t}\right)\frac{\partial F}{\partial W} = 0\,, \tag{6}$$

where $\mathbf{v}_\mathrm{g} \equiv v_\parallel \hat{\mathbf{b}} + \mathbf{v}_\mathrm{d} + \mathbf{v}_\mathrm{E} + (v_\parallel/B)\nabla\langle A_\parallel\rangle \times \hat{\mathbf{b}}$, and

$$\mathbf{v}_\mathrm{d} \equiv \frac{v_\parallel^2 + \mu B}{B^2}\hat{\mathbf{b}} \times \nabla B \qquad \text{and} \qquad \mathbf{v}_\mathrm{E} \equiv \frac{c}{B}\hat{\mathbf{b}} \times \nabla\langle\phi\rangle \tag{7}$$

Split F into $F = F_0 + f$, where F_0 represents the macroscopic equilibrium, and f represents microscopic fluctuations (smaller by one order in ρ_*).

Ignore nonlinearities connected with the third term on the LHS of (6) (down one order in ρ_*).

Model Equations

GENERAL ATOMICS

The equation describing microscopic fluctuations (for each species) is

$$\frac{\partial g}{\partial t} + (v_\parallel \hat{\mathbf{b}} + \mathbf{v}_\mathrm{d}) \cdot \frac{\partial g}{\partial \mathbf{R}} = -\frac{\partial F_0}{\partial W}\frac{\partial \langle U \rangle}{\partial t} - \frac{1}{B}\hat{\mathbf{b}} \times \nabla \langle U \rangle \cdot \nabla (F_0 + g) \qquad (8)$$

where $f = \langle \phi \rangle \, \partial F_0 / \partial W + g$ and $U \equiv \phi - v_\parallel A_\parallel$. The field evolution is subsequently determined by a sum over all species (subscript s) in the gyro-Maxwell equations:

$$-\nabla^2 \phi(\mathbf{x}, t) = 4\pi \sum_\mathrm{s} e z_\mathrm{s} \int d^3 v \left(z_\mathrm{s} e \phi(\mathbf{x}) \frac{\partial F_{0s}}{\partial W} + \langle g \rangle_\mathrm{s} \right), \qquad (9)$$

$$-\nabla^2 A_\parallel(\mathbf{x}, t) = 4\pi \sum_\mathrm{s} e z_\mathrm{s} \int d^3 v \, v_\parallel \langle g \rangle_\mathrm{s} \, . \qquad (10)$$

Above, $\langle g \rangle$ is evaluated at the plasma position $\mathbf{x}$ (consistent to lowest nontrivial order in ρ_* with Hahm, Brizard, etc).

Coordinate System

GENERAL ATOMICS

GYRO uses a real-space coordinate system (r, θ, α), where r is a flux-surface label ($\hat{\mathbf{b}} \cdot \nabla r = 0$), θ is an angle in the poloidal plane, and

$$\alpha \equiv \zeta - \int_0^\theta d\theta \, \hat{q}\,, \tag{11}$$

with $\hat{q} \equiv (\hat{\mathbf{b}} \cdot \nabla\zeta)/(\hat{\mathbf{b}} \cdot \nabla\theta)$ the local safety factor. α is chosen to be constant along a field line ($\hat{\mathbf{b}} \cdot \nabla\alpha = 0$). The parallel derivative in these coordinates is simply $\hat{\mathbf{b}} \cdot \nabla = (\hat{\mathbf{b}} \cdot \nabla\theta)\partial_\theta$. In this article, the bare symbol q is reserved for the flux-surface-averaged safety factor.

$$q \equiv \frac{1}{2\pi} \int_0^{2\pi} d\theta \, \hat{q} \tag{12}$$

Fluctuating Fields

GENERAL ATOMICS

We expand $(\phi, A_{||}, g)$ as Fourier series in α. For example, the electrostatic potential is written

$$\phi = \sum_n \phi_n(r,\theta) e^{-in\alpha} \tag{13}$$

Although the physical field, ϕ, is 2π-periodic in θ, this representation has the implication that the Fourier coefficients, ϕ_n, are nonperiodic, and satisfy the phase condition $\phi_n(r,\pi) = \phi_n(r,-\pi)\ \exp[-2\pi i n q(r)]$.

Since ϕ is real, the coefficients satisfy $\phi_n^* = \phi_{-n}$.

Normalization

GENERAL ATOMICS

dimension	unit	description
Length	a	minor radius
Velocity	c_s	sound speed ($\sqrt{T_e(0)/m_i}$)
Mass	m_i	ion mass
Time	a/c_s	
Temperature	$T_e(0)$	electron temperature

Introduce renormalized densities and distribution functions $\hat{\mathsf{n}}_\mathsf{s}$ and $\hat{g}_\mathsf{s}$ according to $\mathsf{n}_\mathsf{s} = \hat{\mathsf{n}}_\mathsf{s}\mathsf{n}_e(0)$ and $g_\mathsf{s} = \hat{g}_\mathsf{s}\mathsf{n}_e(0)F_\mathsf{s}^M$.

$F_\mathsf{s}^M \equiv e^{-W/T_\mathsf{s}}/(\pi^{3/2}v_\mathsf{s}^3)$ and $T_\mathsf{s}(r) = m_\mathsf{s}v_\mathsf{s}^2/2$.

The equilibrium distribution is $F_{0s} = \mathsf{n}_\mathsf{s}\, F_\mathsf{s}^M$

Velocity Space

GENERAL ATOMICS

The velocity integrals in Eqs. (9) and (10) are rewritten in terms of the energy, W, and pitch angle, $\lambda \equiv \mu/W$.

Use the identity $\sum_\sigma (2\pi)\, dW\, d\lambda = (m^2 v_\parallel / B)\, d^3v$, where $\sigma \equiv \mathrm{sgn}(v_\parallel)$.

For each species, introduce the operator V, such that

$$\int d^3v\, F^M f = \sum_\sigma V^\sigma[f^\sigma] \quad \text{with} \quad V^\sigma[f] \equiv \frac{1}{2\sqrt{\pi}} \int_0^\infty d\epsilon\, e^{-\epsilon} \sqrt{\epsilon} \int_0^1 \frac{d(\lambda B) f^\sigma}{\sqrt{1-\lambda B}}\,, \tag{14}$$

Above, $\epsilon \equiv W/T$ and $\sum_\sigma V^\sigma[1] = 1$.

Misc. Definitions

GENERAL ATOMICS

$$\lambda_{\mathrm{D}} \equiv \sqrt{\frac{T_e(0)}{4\pi n_e(0) e^2}}, \qquad \beta_e \equiv \frac{n_e(0) T_e(0)}{B_0^2/8\pi}, \qquad \rho_{\mathrm{s}} \equiv \frac{c_s}{eB_0/m_i c}. \tag{15}$$

For simple $s-\alpha$ equilibrium, we have

$$\omega_* \equiv k_\theta \rho_s \left[\frac{1}{L_n} + (\epsilon - 3/2)\frac{1}{L_T}\right] \tag{16}$$

$$\omega_{\mathrm{d}}^{(1)} \equiv k_\theta \rho_s \frac{2zT}{R_0}\epsilon\left(1 - \frac{\lambda\hat{B}}{2}\right)\left[\cos(\theta) + (s\theta - \alpha\sin\theta)\sin(\theta)\right] \tag{17}$$

$$\omega_{\mathrm{d}}^{(r)} \equiv -i\rho_s \frac{2zT}{R_0}\epsilon\left(1 - \frac{\lambda\hat{B}}{2}\right)\sin\theta \tag{18}$$

$$u_\parallel \equiv \frac{v_\parallel}{qR_0} \tag{19}$$

$$\hat{B} \equiv \frac{1}{1 + r/R_0\cos\theta} \tag{20}$$

Time-Advance Algorithm

GENERAL ATOMICS

Because we are solving a multidimensional PDE, and wish to take relatively large timesteps, we resort to operator splitting. This allows us to treat substeps with implicit or high-order explicit methods.

One full timestep constitutes the cycle: **collision step** $\rightarrow$ **nonlinear step** $\rightarrow$ **radial step** $\rightarrow$ **poloidal step with field solve**. While each of the substeps modifies g, only the poloidal step involves a change in ϕ. In this newsec we give only a description of the continuous equations solved at each substep. The collision step, which solves for the response due to pitch-angle scattering, is not discussed for the sake of brevity. Moreover, the length of the present paper allows only an outline of the numerical methods, discretized equations and parallelization algorithms used in *GYRO*.

Nonlinear Step

GENERAL ATOMICS

We make a partial advance using the nonlinear terms only. In the ballooning limit, with circular flux surfaces, the equation to be solved is

$$\partial_t \hat{g}_n = \frac{i\rho_s q}{r} \sum_{n'} \left[n \langle \hat{U} \rangle_{n'} \partial_r \hat{g}_{n-n'} - n' \partial_r \left(\hat{g}_{n'} \langle \hat{U} \rangle_{n-n'} \right) \right] \tag{21}$$

The discretization scheme, to a very good approximation, is designed to satisfy the following entropic conservation law:

$$\frac{\partial}{\partial t} \int d\alpha \int dr \, |\hat{g}|^2 \rightarrow \frac{\partial}{\partial t} \sum_n \int dr \, |\hat{g}_n|^2 \sim \mathcal{O}(\Delta t^4) \tag{22}$$

Centered finite differences and the conservative form, Eq. (21), are essential to obtain Eq. (22). In practice, at least five-point (fourth-order) rules are used. The system of ordinary equations is then advanced in time using a 4th-order RK method. Entropy is conserved to $\mathcal{O}(\Delta t)^5$ in one nonlinear step.

Radial Step

GENERAL ATOMICS

The radial step ignores all but radial derivatives contained in the linear terms. Physically, this accounts for the physics connected with the radial derivative, $\omega_{\mathrm{d}}^{(r)}\partial_r$, in the curvature drift, $\omega_{\mathrm{d}} = \omega_{\mathrm{d}}^{(1)} + \omega_{\mathrm{d}}^{(r)}\partial_r$

$$\partial_t \widehat{g} = i\omega_{\mathrm{d}}^{(r)}\,\partial_r \widehat{g} \tag{23}$$

When $\omega_{\mathrm{d}}^{(r)}$ is held fixed at the central radius (*i.e.*, the ballooning limit), solve the equation using a forward and backward Fourier transform in r. This method has the added benefit that at no extra expense we can add hyperviscosity to eliminate the effects of electron Landau resonances in the electron kinetic equation. Banded-diagonal solvers are used in the nonperiodic case where radial variation is accounted for.

Poloidal Step

GENERAL ATOMICS

The poloidal step ignores derivatives with respect to pitch angle, energy and radius. Nonlinearities are also neglected. We use a phase-space conserving differencing scheme to avoid passing-particle instability of $n = 0$ modes. The normalized equations are

$$\left(\partial_t + u_{\parallel}\partial_\theta\right)\hat{g} = \hat{\alpha}\partial_t\langle\hat{U}\rangle + i\omega_{\rm d}^{(1)}\hat{g} - i\hat{\rm n}\omega_*\langle\hat{U}\rangle\,, \tag{24}$$

$$\lambda_{\rm D}^2\,\nabla^2\phi + \sum_{\rm s} z_{\rm s}\sum_{\sigma} V^{\sigma}[\langle\hat{g}\rangle_{\rm s}^{\sigma}] + \sum_{\rm s} z_{\rm s}\hat{\alpha}_{\rm s}\phi = 0 \tag{25}$$

$$\frac{2\rho_{\rm s}^2}{\beta_e}\,\nabla^2 A_{\parallel} + \sum_{\rm s} z_{\rm s}\sum_{\sigma} V^{\sigma}[v_{\parallel}\langle\hat{g}\rangle_{\rm s}^{\sigma}] = 0\,, \tag{26}$$

with $\hat{\alpha} \equiv z\hat{\rm n}/T$. These equations are solved implicitly for both electrons and ions to yield a partial advance of $\hat{g}$ and $(\phi, A_{\parallel})$. An implicit field-solve is used to avoid the Courant limit on timestep imposed by the electron parallel operator $\left(\partial_t + u_{\parallel}\partial_\theta\right)\hat{g}_e$.

Radial Grid

GENERAL ATOMICS

For a given choice of equilibrium and reference mode number $n^{\rm ref}$, ballooning modes oscillate at wavelengths $k_r = (p + \ell/\ell_*)k_*$, where $k_* \equiv 2\pi s k_\theta^{\rm ref}$ and $k_\theta^{\rm ref} = n^{\rm ref} q/r$. A given mode has a fixed integer values of ℓ, with $0 \leq \ell < \ell_*$, and runs over all integral values of p. The most unstable mode has $\ell = 0$, and more stable modes $\ell > 0$.

Knowing k_* and ℓ_*, we set the box length at $L = 2\pi\ell_*/k_*$. Numerically, we retain only a finite number of p-values for each mode ($|p| \leq j_*$), since the partial contribution to the eigenmode drops off rapidly with each successive p. Then, the number of radial gridpoints required to describe ℓ_* ballooning modes at $n = n^{\rm ref}$ is $n_r = 2j_*\ell_* + 1$.

Radial Grid

GENERAL ATOMICS

A value for ρ_s is also required – typically, we choose $k_\theta^{\rm ref}\rho_s \sim 0.3$. Experience shows that for $s \sim 1$, it is generally sufficient to choose five k's per ballooning mode ($j_* = 2$), or equivalently $n_r = 4\ell_* + 1$, where n_r is the number of radial gridpoints.

A linear calculation of only the most unstable mode requires $\ell_* = 1$. Nonlinear runs typically require $\ell_* = 24$ (and at least ten values of n) for proper saturation. A crucial feature of the code is that the code timing and storage increase linearly with n_r. This is a result of banding methods which make use of the localized nature of gyroaverages and derivatives in a realistic simulation box.

Numerical problems

GENERAL ATOMICS

There are numerous difficulties associated with a real-space radial grid. The most was connected with $n = 0$ field-solve matrix – used in the poloidal step. This matrix has a null eigenvalue for $k_r = 0$. Although we do not evolve the equilibrium ($k_r = 0, n = 0$), the smallest values of k_r used in nonlinear simulations are prone to numerical instability which appears as a result of the split radial and poloidal steps. We have cured this instability using

- ▷ a conservative differencing scheme for Eq. (24)
- ▷ a two-stage (predictor-corrector type) method to improve the accuracy of the total linear step (radial plus poloidal). This ensures to high accuracy the balance between the terms $i\omega_{\mathrm{d}}^{(r)}\,\partial_r \widehat{g}$ and $u_{||}\partial_\theta \widehat{g}$ for $n = 0$.

Numerical Results

GENERAL ATOMICS

To benchmark *GYRO* for finite-n ballooning modes, we used the linear electromagnetic solver *GKS* [Kotschenreuther]. The validity of *GKS* has been rigorously established. The simulation results presented generally share a common set of input parameter values (table below). When exceptions occur, they are indicated. Below, n_ϵ is the number of energy gridpoints, n_λ is the number of pitch angle gridpoints, and n_θ is the number of gridpoints in poloidal angle. Because we multipoint methods for radial integration and differentiation, we obtain much better than second order accuracy.

parameter	value	parameter	value	parameter	value
R/a	3.0	r/a	0.5	a/L_T	3.0
a/L_N	1.0	s	1.0	q	2.0
n_ϵ	5	n_λ	26	n_θ	32

Numerical Results

GENERAL ATOMICS

Electrostatic adiabatic electron case We perform one *GYRO* run with a fine radial grid ($n_r = 97$), 15 toroidal modes ($n = 0, 5, 10, \ldots, 70$), and adiabatic electrons. The k_y-spectrum is $k_\theta \rho_s = 0.0, 0.05, 0.1, \ldots, 0.7$. Results agree with *GKS*.

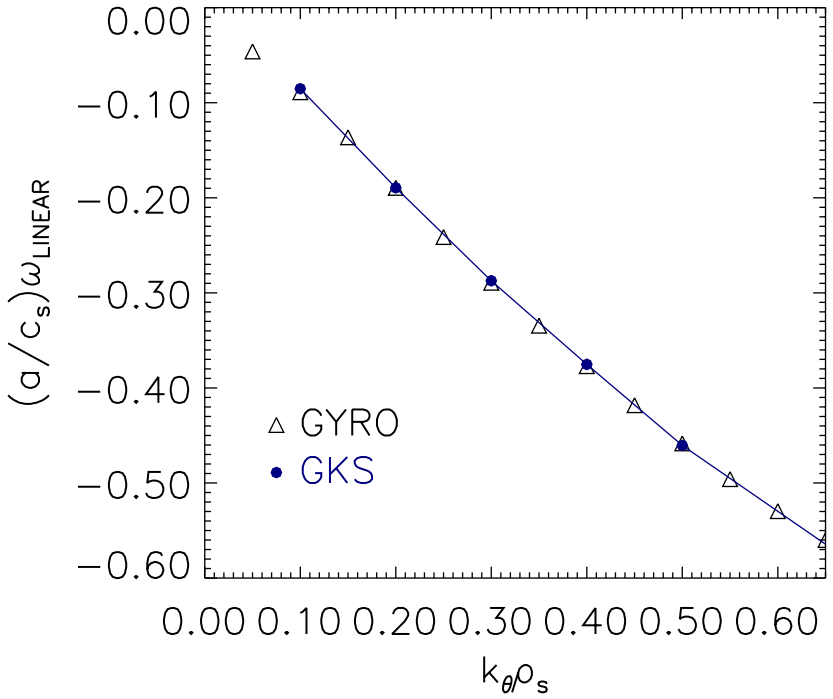

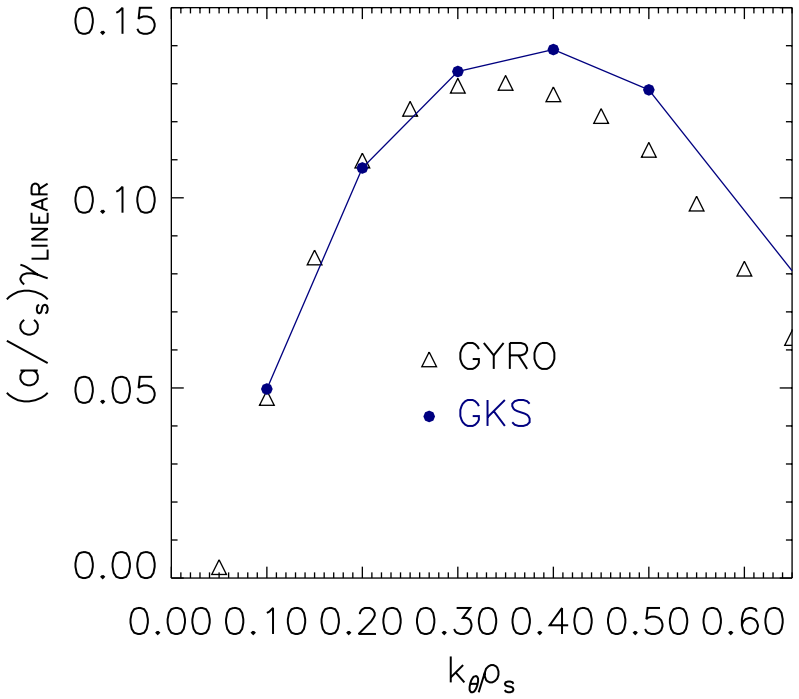

Numerical Results

GENERAL ATOMICS

Electromagnetic ballooning modes *GYRO* is not a ballooning code, but it's possible to reconstruct an equivalent ballooning-space solution from the real-space one. The largest k_r is damped to mimic the *GKS* boundary condition, which eliminates the electron layer response.

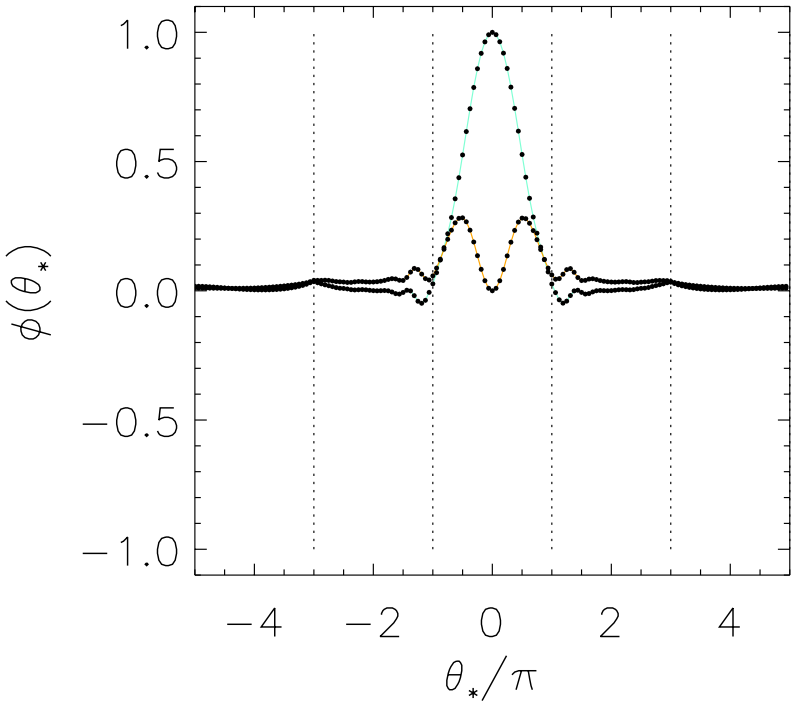

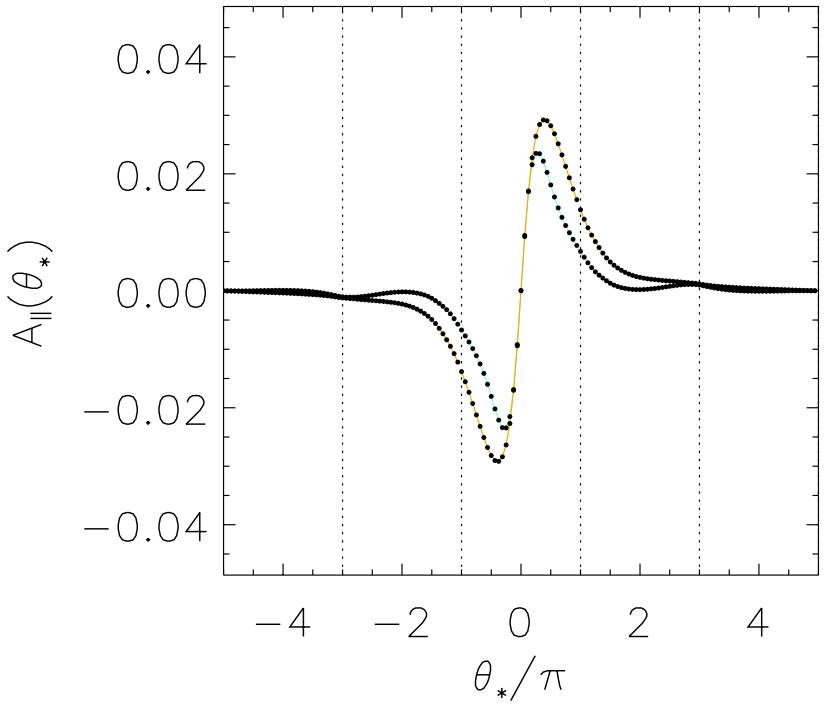

Numerical Results

GENERAL ATOMICS

Electrostatic nonadiabatic electron parameter scan We use the full nonlinear grid and do a scan of linear eigenmodes: ($n_r = 97$), $n_n = 15$, box length $L = 80\rho_s$. The results are very close to *GKS* runs on case-dependent grids.

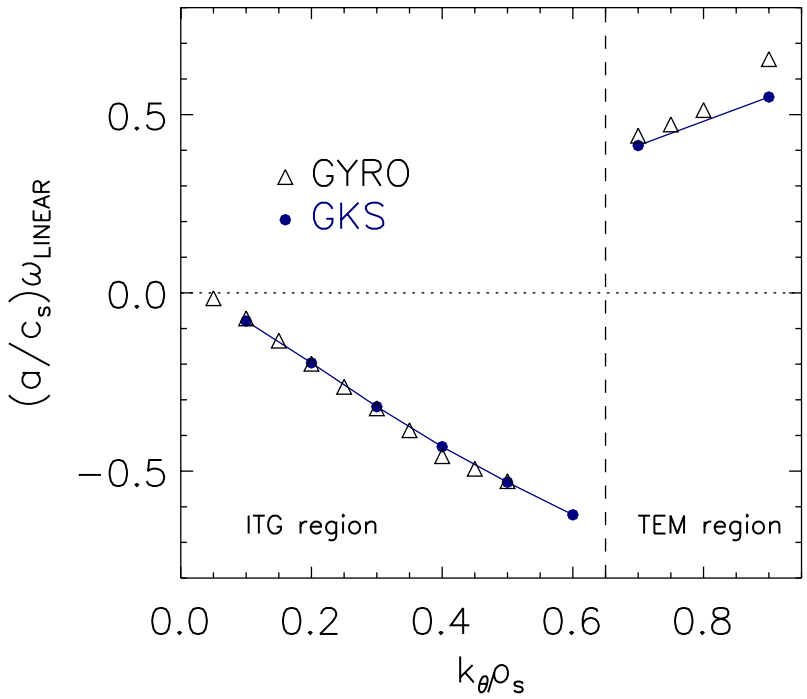

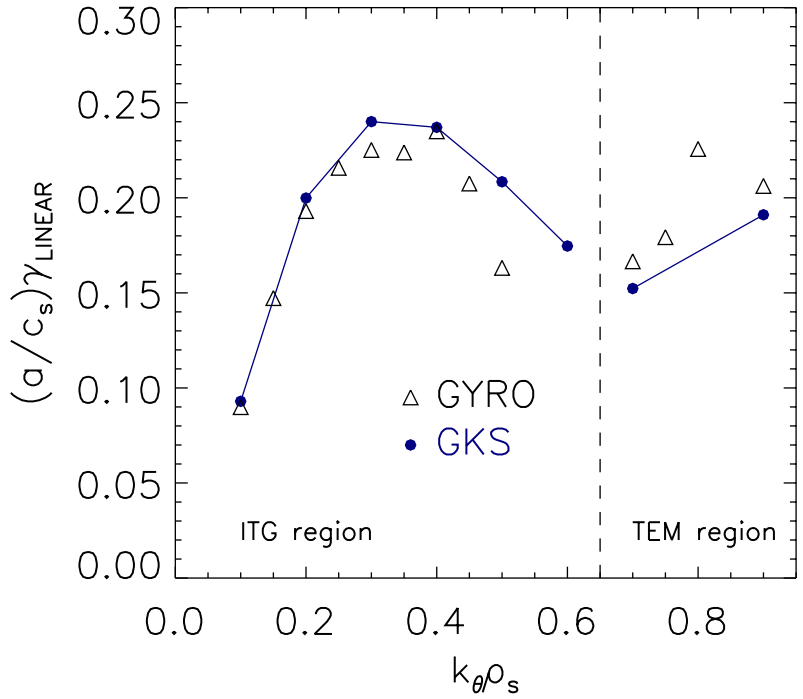

Numerical Results

GENERAL ATOMICS

Axisymmetric modes We can test the accuracy of axisymmetric poloidal flow decay for $n = 0$ modes. Results are in exact agreement with Rosenbluth-Hinton theory.

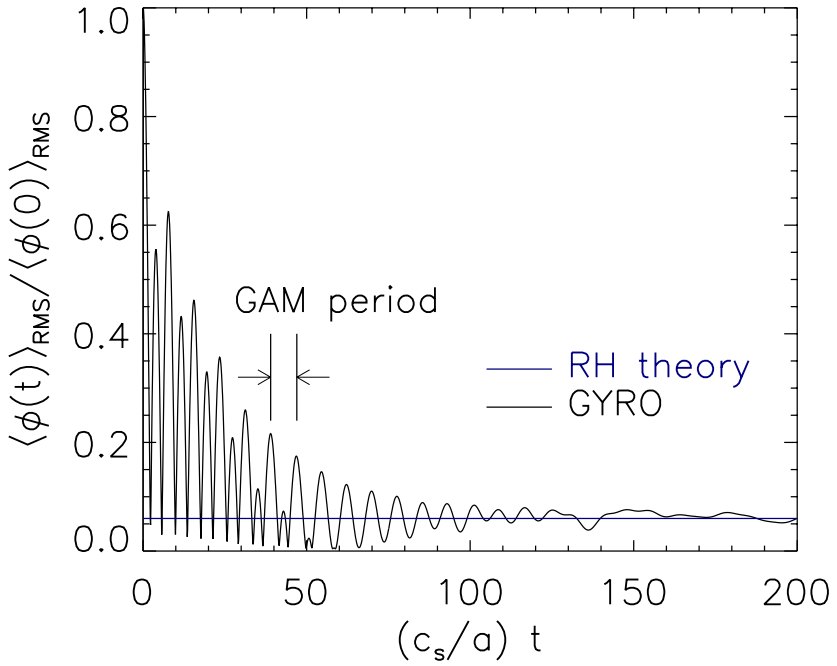

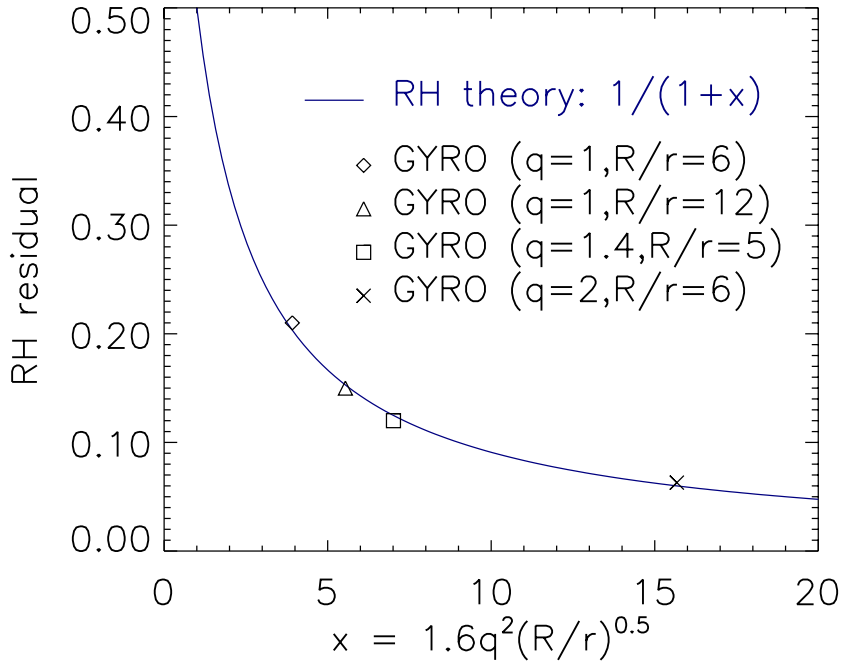

Nonlinear ITG

GENERAL ATOMICS

GYRO fully operational for nonlinear, kinetic ions (ITG). We set the grid resolution at $n_r = 97$, $L = 80\rho_s$, $n_\theta = 16$, $n_\lambda = 14$, $n_n = 14$, $k_\theta \rho_s = 0, 0.06, \ldots, 0.78$ and use $(c_s/a)\Delta t = 0.1$.

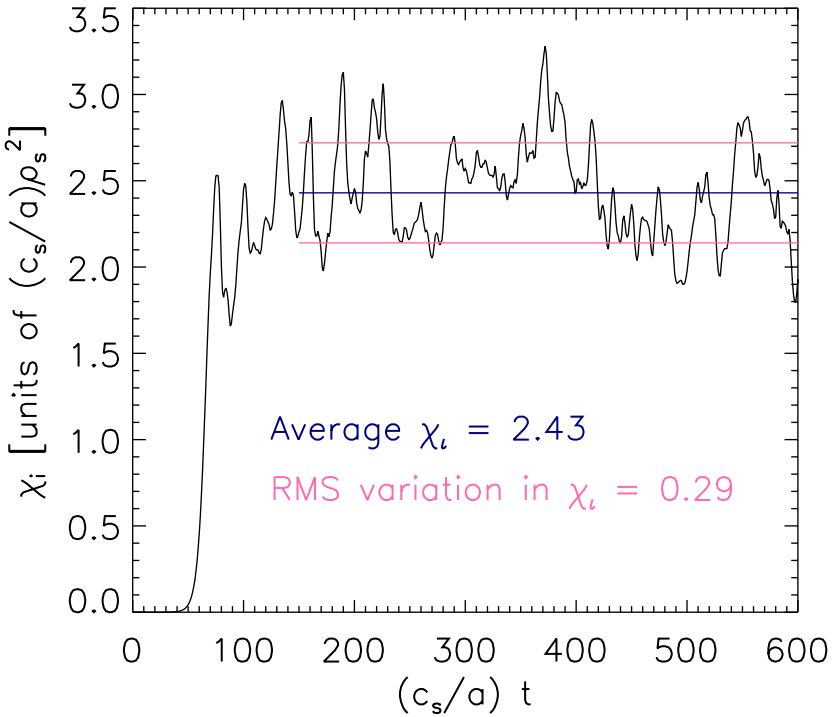

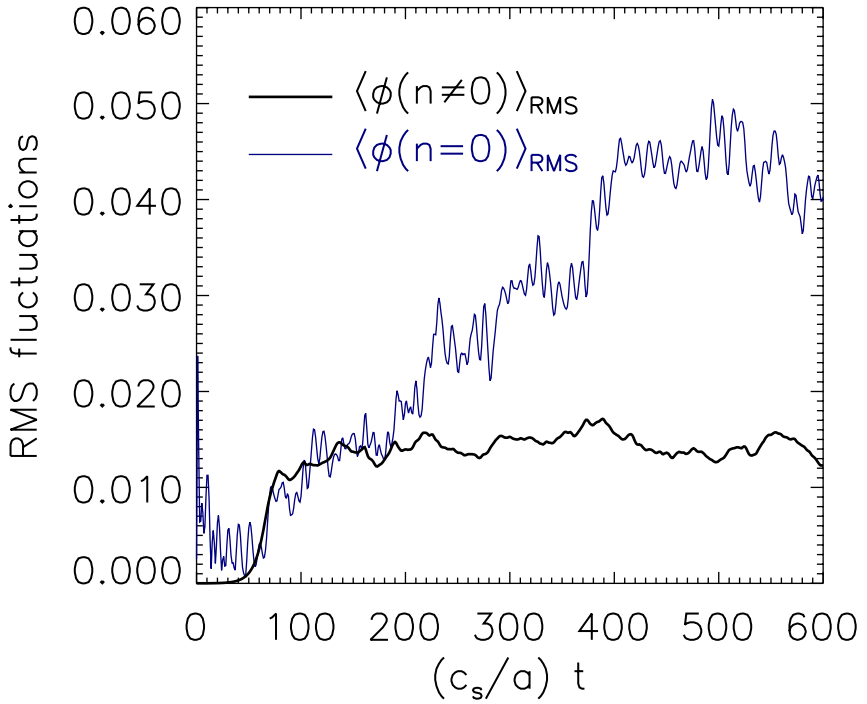

Nonlinear ITG

GENERAL ATOMICS

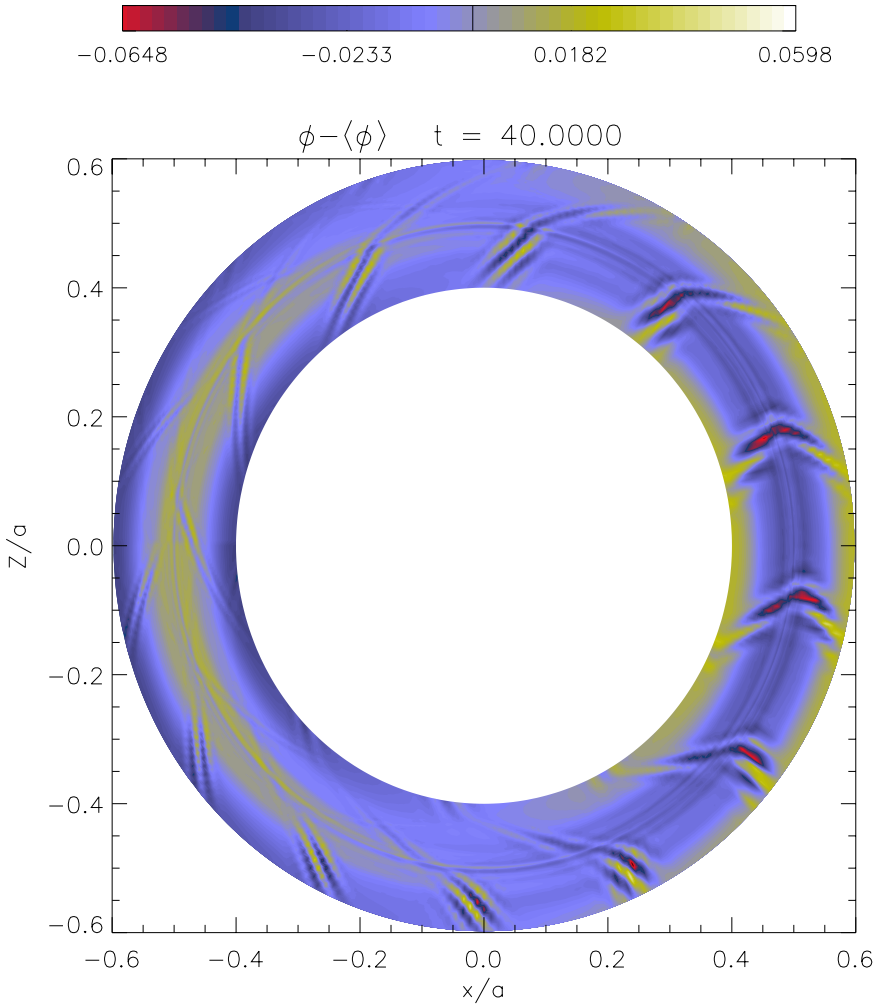

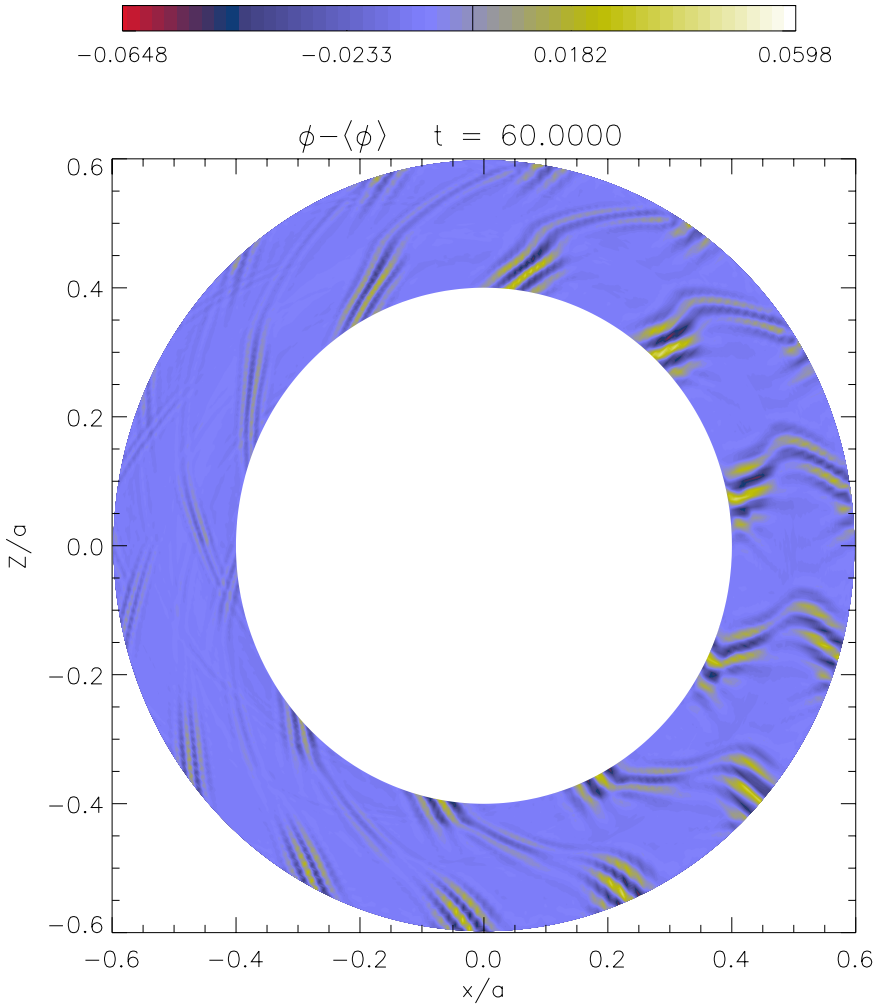

/u/candy/gyro/sim/n14mrky.78_iPCd.col.0nodampVldt.10sNLb4 [0.1.12] [Mon Oct 16 01:05:49 PDT 2000] /u/candy/gyro/sim/n14mrky.78_iPCd.col.0nodampVldt.10sNLb4 [0.1.12] [Mon Oct 16 01:05:49 PDT 2000]

Nonlinear ITG

GENERAL ATOMICS

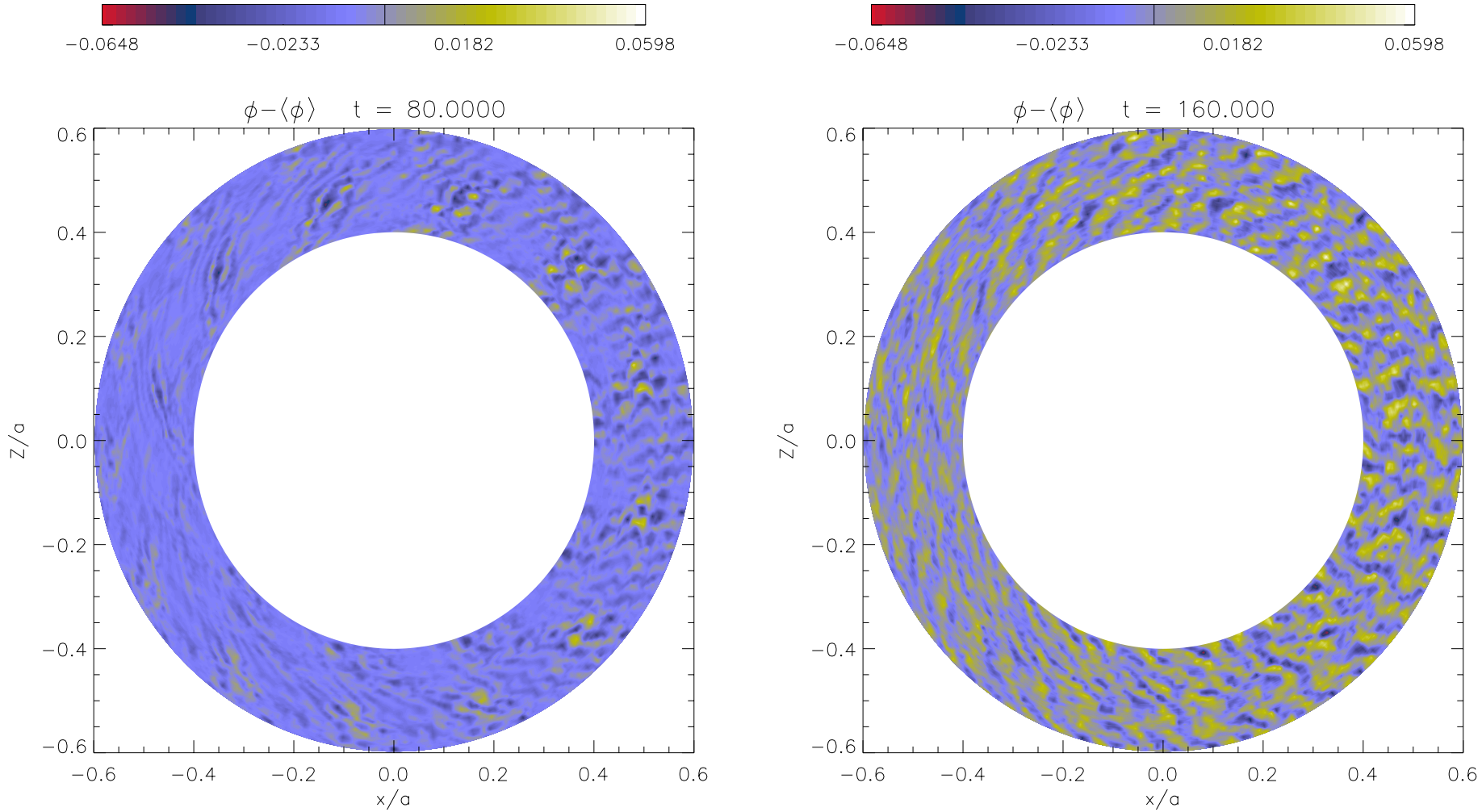

/u/candy/gyro/sim/n14mrky.78_iPCd.col.0nodampVldt.10sNLb4 [0.1.12] [Mon Oct 16 01:05:49 PDT 2000] /u/candy/gyro/sim/n14mrky.78_iPCd.col.0nodampVldt.10sNLb4 [0.1.12] [Mon Oct 16 01:05:49 PDT 2000]

Code Performance

GENERAL ATOMICS

GYRO scales well up to the full capacity of the NERSC IBM RS/6000 SP and CRAY T3E-900 machines, as well as the GA Intel Beowulf clusters. The maximum performance on the larger GA *STELLA* cluster averages about 1/10th that of the full IBM SP.

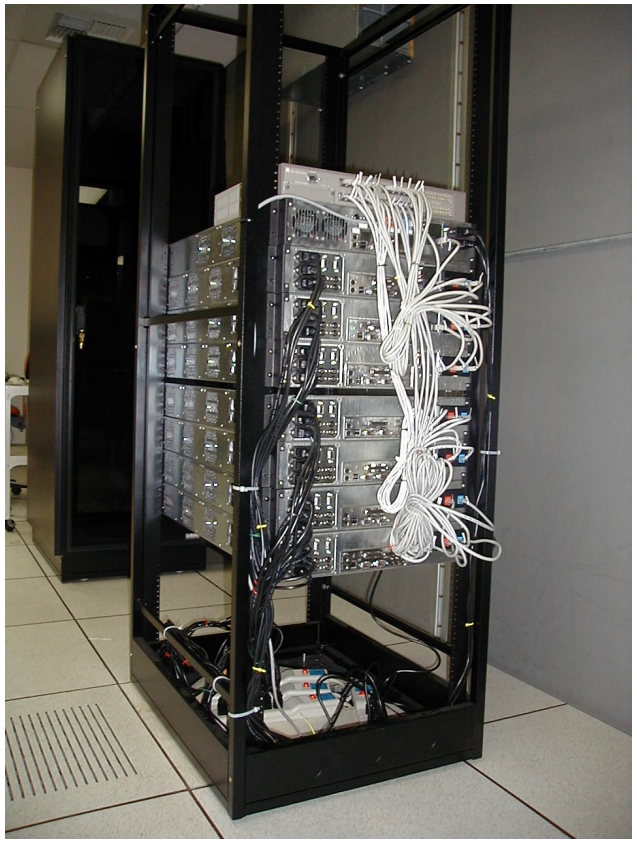

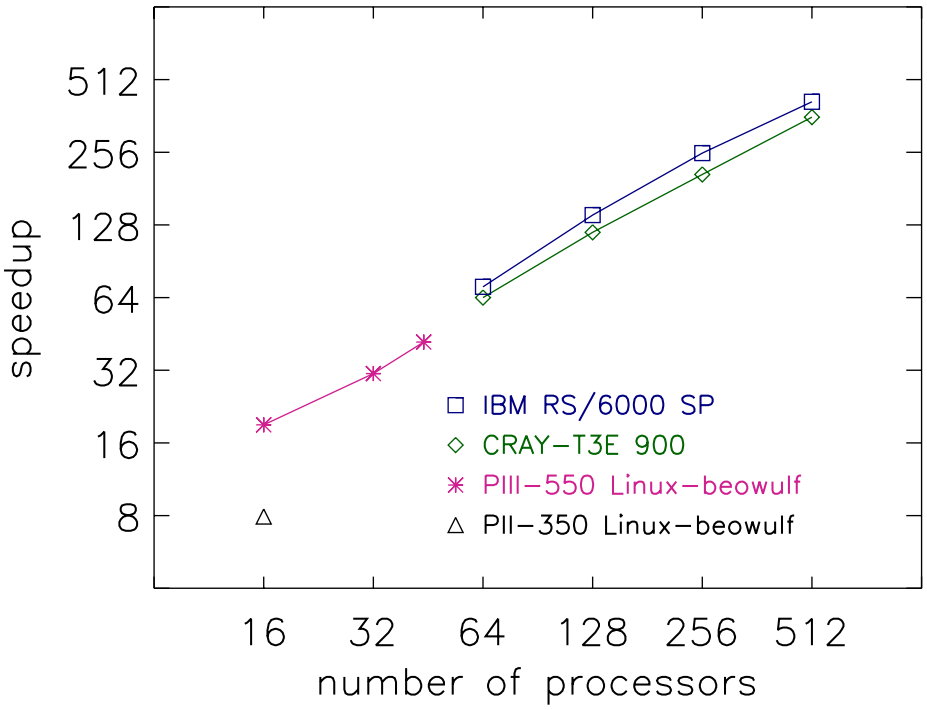

Progress and Conclusions

GENERAL ATOMICS

Numerical benchmarking demonstrates that *GYRO* operates correctly and efficiently in flux-tube mode, carrying with it the heavy infrastructure required for full-radius operation.

The use of banded multi-point methods for gyroaverages, nonlinear derivatives and field-solves allows linear-in-n_r code scaling.

Linear, electromagnetic comparisons with *GKS* show very good agreement.

$n = 0$ modes behave in accordance with Rosenbluth-Hinton theory.

Results from nonlinear simulations give thermal diffusivities in rough agreement with *GS2*.